JOURNAL OF GEOPHYSICAL RESEARCH, VOL. 112, D20108, doi:10.1029/2006JD008206, 2007

Radar-based quantitative precipitation estimation over Mediterranean and dry climate regimes

Efrat Morin[1] and Marco Gabella[2]

Received 30 October 2006; revised 10 May 2007; accepted 24 July 2007; published 20 October 2007.

[1] Quantitative precipitation estimation based on meteorological radar data potentially provides continuous, high-resolution, large-coverage data that are essential for meteorological and hydrologic analyses. While intense scientific efforts have focused on precipitation estimation in temperate climatic regimes, relatively few studies examined radar-based estimates in dry climatic regions. The paper examines radar-based rain depth estimation for rainfall periods (a series of successive rainy days) in Israel, where the climate ranges between Mediterranean to dry. Three radar-gauge adjustment methods are compared: a one-coefficient bulk adjustment, which simply removes the mean bias; a two-coefficient range adjustment based on a weighted regression (WR); and a four-coefficient adjustment based on a weighted multiple regression (WMR), which assumes a locally varied, nonisotropic correction factor. The WMR technique has been previously applied in the Alps of Europe. Adjustment coefficients have been derived for 28 rainfall periods using 59 independent gauges of a quality-checked training data set. The validation was based on an independent data set composed of gauges located in eleven 20×20 km^2 validation areas, which are representative of different climate, topography and radar distance conditions. The WR and WMR methods were found preferable with a slight better performance of the latter. Furthermore, a novel approach has been adopted in this study, whereby radar estimates are considered useable if they provide information that is better than gauge-only estimates. The latter was derived by spatial interpolation of the gauges belonging to the training data set. Note that these gauges are outside the validation areas. As for the radar-adjusted estimates, gauge-derived estimates were assessed against gauge data in the validation areas. It was found that radar-based estimates are better for the validation areas at the dry climate regime. At distances larger than 100 km, the radar underestimation becomes too large in the two northern validation areas, while in the southern one radar data are still better than gauge interpolation. It is concluded that in ungauged areas of Israel it is preferable to use WMR-adjusted (or alternatively, simply WR-adjusted) radar echoes rather than the standard bulk adjustment method and for dry ungauged areas it is preferable over the conventional gauge-interpolated values derived from point measurements, which are outside the areas themselves. The WR and WMR adjustment methods provide useful rain depth estimates for rainfall periods for the examined areas but within the limitation stated above.

Citation: Morin, E., and M. Gabella (2007), Radar-based quantitative precipitation estimation over Mediterranean and dry climate regimes, *J. Geophys. Res.*, *112*, D20108, doi:10.1029/2006JD008206.

1. Introduction

[2] Accurate quantitative precipitation estimation (QPE) is one of the most important elements in meteorological and hydrologic analyses. It has been long recognized, however, that rain gauge networks are usually inadequate because of their limited sampling distribution. During the last decades intense scientific efforts have been devoted to utilize remote sensing information for the estimation of high-resolution precipitation data over large areas. Ground-based meteorological radar systems are the most common source of this information.

[3] While a considerable number of papers deal with radar-based precipitation estimation in temperate climatic regimes, few have focused on dry climatic regions [e.g., *Morin et al.*, 2005]. According to the Köppen classification these dry regions occupy more than a quarter of the world's land area (more than any other major climatic type) with typically meager, irregular and highly variable precipitation [*Ahrens*, 2003; *Goodrich et al.*, 1995]. The great spatial variability of rainfall in such regions, compounded by fewer settlements and isolation, means that dense manual rain

[1]Department of Geography, Hebrew University of Jerusalem, Jerusalem, Israel.
[2]Dipartimento di Elettronica, Politecnico di Torino, Turin, Italy.

0148-0227/07/2006JD008206$09.00

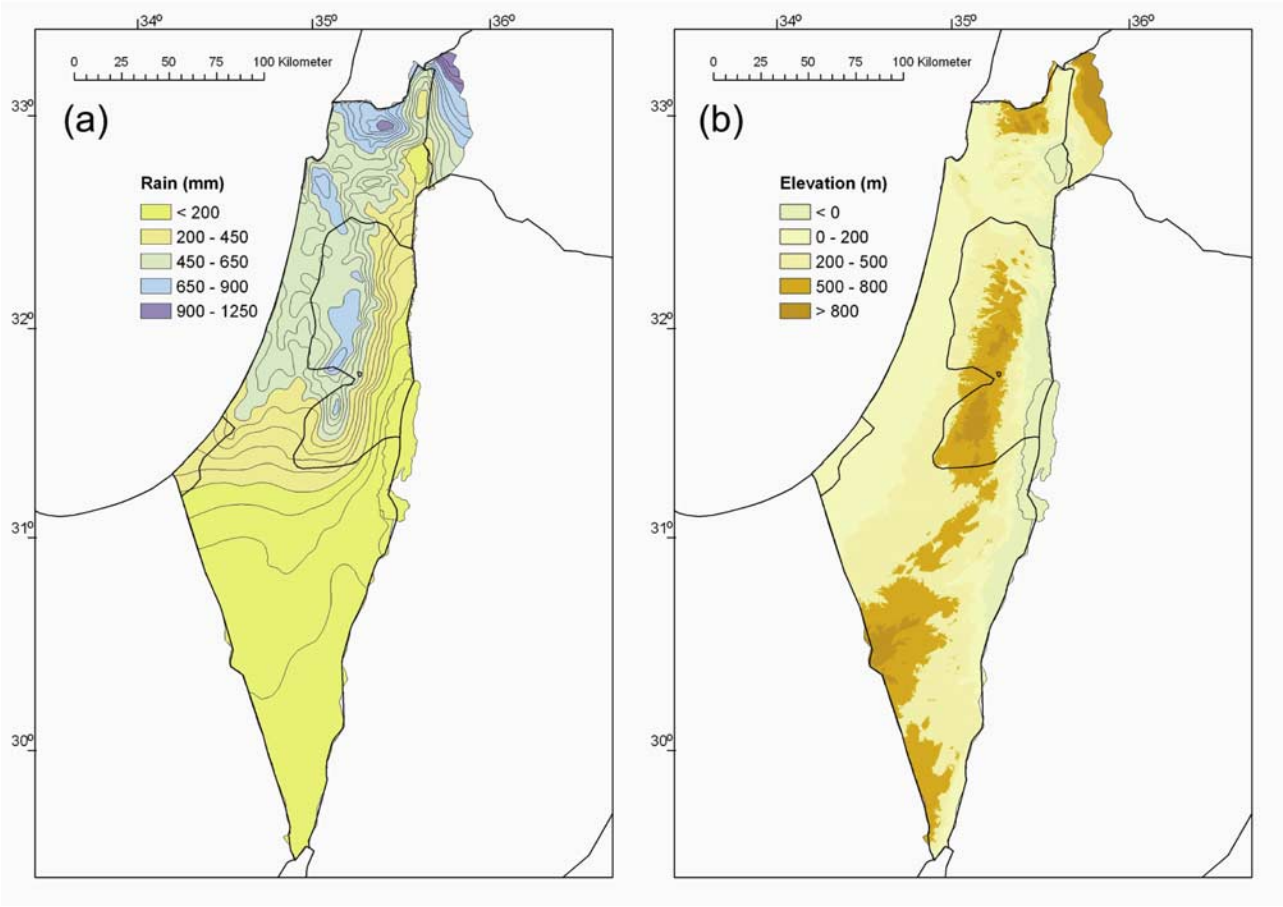

Figure 1. (a) Climatological annual rainfall (30-a average) over Israel and (b) topography of Israel.

gauge networks cannot be established and that recording stations will be too expensive to establish and maintain [e.g., *Michaud and Sorooshian*, 1994]. Therefore the advantage of radar-based QPE in dry climate regimes is potentially large and should be thoroughly investigated.

[4] This is the objective of the present study: to examine methods for radar-based QPE of accumulated rain depth during rainfall periods in Israel, where the climate ranges from Mediterranean to dry. This goal is achieved using radar-gauge training and validation procedures applied to a long rainfall data set of 5-a duration.

1.1. Work of the Past: Radar Adjustment in Nordic and Midlatitude Regions

[5] Radar-based QPE are subject to several sources of errors. Among them is the effect of topography causing ground clutter contamination and beam blockage, especially in mountainous regions, beam broadening and its increasing altitude above ground with distance, and gradients of vertical reflectivity profiles [e.g., *Joss and Waldvogel*, 1990; *Germann and Joss*, 2004]. Rain gauges are usually considered to provide accurate "point" measurements. In this context, "point" means a gauge cross section typically of 200 cm^2 (and a sampling volume of the order of $\sim$30 m^3 every 5 min, assuming 1 mm diameter raindrops). Consequently, it is well known that gauge observations represent local effects and not areal quantities. Therefore for hydrological applications, in which areal precipitation measurements are needed, their main drawback is undersampling [e.g., *Kitchen and Blackall*, 1992; *Krajewski and Smith*, 2002; *Krajewski et al.*, 2003], i.e., not enough observations to describe the variability of the field. Because of the spatial variability of rainfall, it is obvious that point measurements would undersample the precipitation fields, even though the measurements themselves are correct. Radar measurements can add the desired information on the areal distribution of precipitation. Several methods have been developed over the last decades to merge radar estimates with gauge measurements, so as to obtain quantitatively accurate and spatially continuous radar-derived precipitation fields [e.g., *Wilson*, 1970; *Brandes*, 1975; *Caine and Smith*, 1976; *Wilson and Brandes*, 1979; *Collier et al.*, 1983; *Collier*, 1986; *Smith and Krajewsky*, 1991; *Seo et al.*, 2000]. Many of these analyzed the radar-to-gauge ratio. *Koistinen and Puhakka* [1981] proposed a range-dependent adjustment based on a multiple regression between the radar-to-gauge ratio on a decibel scale and the linear and squared distance. In mountainous terrain the radar-gauge distance is not sufficient as a predictor, since other factors such as beam shielding by relief and orography also play a (negative) role on radar estimates. To cope with this kind of problem *Gabella et al.* [2001] proposed an adjustment based on a weighted multiple regression (WMR). The weighted regression is performed in the logarithmic domain of the variables,

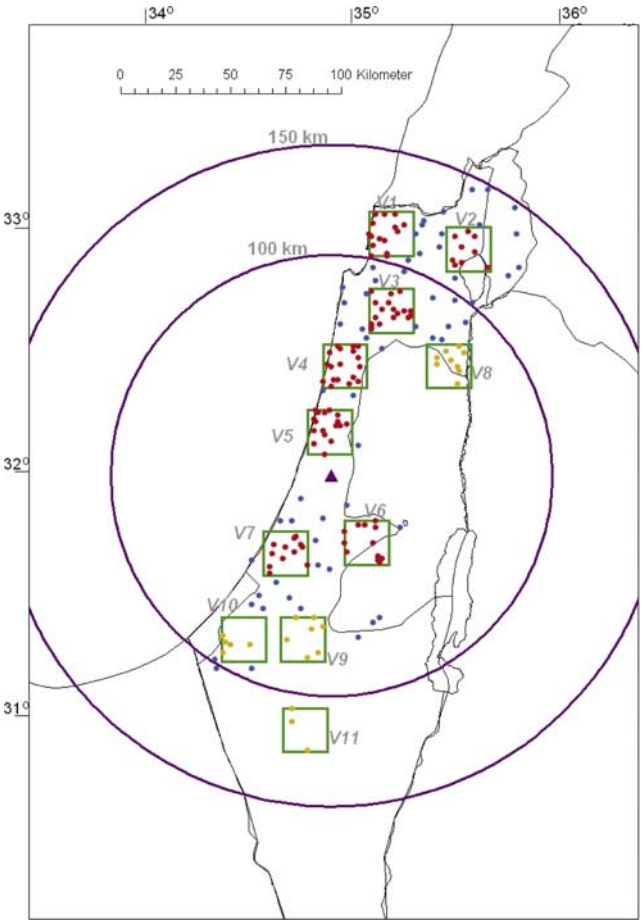

Figure 2. Rain gauges (solid circles) and the eleven validation areas of 20 × 20 km^2 size (marked by V1–V11). Radar location is marked by a triangle, and the 100 and 150 km radiuses are indicated.

where power laws lead to linear relationships. With respect to *Koistinen and Puhakka* [1981], the WMR is based on the same dependent variable; however the independent variables are rather the logarithm of the distance, Log$D$, the minimum height a meteorological target must reach over the gage to be visible to the radar, HV, and the height of the ground (H). The first variable reflects the effects of beam broadening, nonhomogeneous filling of the pulse volume and overshooting, coupled with the influence of the vertical profile of reflectivity, which are also reflected in HV. The last variable (H) reflects the depth of the layer where precipitation increases related to orography can occur.

1.2. New Attempts: Radar Adjustment in Mediterranean and Dry Regions

[6] The explanatory variable HV has proved to be particularly effective in mountainous terrain such as the Alps and when using full volume 3-D radar data (see section 3.3 for more details and references). In contrast, in the present study radar-derived precipitation amounts are based on a single elevation (that, however, is not the same in the whole domain, see section 3.2 for details) while the terrain where gauges are available is less complex than the Alps. Hence there is more codependence between HV and Log$D$ (earth curvature and atmospheric refraction). In an ''ideal'' flat region with standard refractivity, in fact, HV could be approximated simply by the square of the distance divided by twice the equivalent Earth's radius. For this reason, we considered substituting HV with another variable that could be correlated with the height of the zero degree isotherm: the latitude. This modified form of the WMR is described in section 3.

2. Description of the Study Region

[7] Israel is located at the southeast corner of the Mediterranean Sea between latitudes 29.5–33.5°N. The climate varies from Mediterranean to dry. Dry climate is characterized by potential evapotranspiration that exceeds precipitation while Mediterranean one has mild wet winter followed by hot and rainless summer. Annual rainfall in Israel is sharply varied from over 1000 mm in the north to only 30 mm in the south, all within a 400 km distance (Figure 1a). Almost half of Israel area has less than 200 mm annual rainfall. The rainy season occurs between October and May and June to September is dry. Generally speaking, annual rainfall amounts increase with latitude and elevation and decreases with distance from the coast. Rainfall originates mostly from cold fronts and the air masses that follow these fronts, which are associated with midlatitude cyclones during their eastward passage over the eastern Mediterranean [*Goldreich*, 2003]. Other rainfall events are associated with the Red Sea Trough, which is a system of tropical origin that may cause high-intensity rainfall mainly during autumn and spring [*Kahana et al.*, 2002].

[8] Israel's physiography consists of three main longitudinal strips: the coastal plain, the hilly region (Galilee, Samaria and Judean Mountains), and the Jordan Rift valley (Figure 1b). The average altitude of the hilly region is about 600 m, while northern Israel has pockets of elevation exceeding 800 m. The Jordan Rift valley, part of the Syrian–East African Rift, is dominated by the Jordan River, the Sea of Galilee and the Dead Sea. The latter, at 399 m below sea level, is the lowest point in the world.

3. Data and Methods

3.1. Data

[9] Radar and rain gauge data for the five hydrological years 1998/1999–2002/2003 were analyzed for this study. Data of the C-band radar system located at Ben-Gurion international airport (close to Tel Aviv) were obtained from E.M.S Mekorot (triangle in Figure 2). Radar data resolutions are 5 min in time and 1.4° × 1 km in space (polar coordinates). Radar scans are at about 13 elevation angles where the first elevation angle is typically at the range of 0.6–1°, the second at 1.4–1.7°, and the third at 2.3–2.5°. Daily gauge rain depth data were obtained from the Israel Meteorological Service and included gauges located within the radar coverage operating during the entire 5 a period (Figure 2).

[10] In the present study, analysis is based on accumulated rain depth during rainfall periods, where rainfall periods are defined as periods of successive rainy days separated by at least one day with no record of rainfall in Israel. Rainfall periods with low accumulated rain depth (less than 10 mm rain depth, average of all gauges) or with large radar data gaps

Table 1. Characteristics of Rainfall Periods Derived From *N* Rain Gauges

Rainfall Period	From	To	*N*	Mean, mm	Min, mm	Max, mm	Std, mm
1	14 Dec 1998	1 Jan 1999	199	77.1	0.2	284.4	64.1
2	12 Dec 1999	15 Dec 1999	193	34.1	0.4	92.3	19.9
3	24 Dec 1999	27 Dec 1999	192	11.0	0.3	33.5	6.7
4	1 Jan 2000	12 Jan 2000	199	111.0	1.1	227.9	40.4
5	14 Jan 2000	2 Feb 2000	199	164.4	16.3	317.0	60.6
6	5 Feb 2000	6 Feb 2000	167	3.9	0.1	18.7	3.8
7	12 Feb 2000	17 Feb 2000	194	49.7	0.3	107.5	23.0
8	7 Dec 2000	26 Dec 2000	202	106.2	10.1	165.3	30.7
9	2 Jan 2001	6 Jan 2001	190	8.3	0.1	31.9	5.8
10	16 Jan 2001	25 Jan 2001	199	79.9	17.1	168.6	30.2
11	3 Feb 2001	9 Feb 2001	197	34.1	2.8	78.6	13.3
12	13 Feb 2001	24 Feb 2001	197	53.2	2.9	105.9	17.8
13	15 Nov 2001	17 Nov 2001	181	8.5	0.1	50.2	8.3
14	25 Nov 2001	27 Nov 2001	187	12.4	0.4	52.6	9.3
15	29 Nov 2001	9 Dec 2001	204	147.1	1.2	416.8	70.5
16	12 Dec 2001	15 Dec 2001	198	15.5	0.1	46.5	9.8
17	18 Dec 2001	21 Dec 2001	195	27.3	3.8	59.3	13.7
18	2 Jan 2002	16 Jan 2002	201	125.3	12.3	234.5	43.5
19	19 Jan 2002	23 Jan 2002	199	35.2	3.8	93.0	16.3
20	27 Jan 2002	30 Jan 2002	200	16.7	1.7	40.7	8.0
21	12 Mar 2002	22 Mar 2002	177	25.5	0.2	124.8	23.9
22	25 Mar 2002	7 Apr 2002	198	74.8	7.1	166.2	33.2
23	23 Nov 2002	25 Nov 2002	191	6.4	0.3	25.5	4.9
24	8 Dec 2002	12 Dec 2002	200	48.1	6.3	121.0	21.2
25	15 Dec 2002	27 Dec 2002	200	131.2	14.8	269.3	37.2
26	13 Jan 2003	23 Jan 2003	200	41.1	6.2	115.9	16.2
27	27 Jan 2003	30 Jan 2003	147	48.4	0.2	171.9	46.1
28	1 Feb 2003	27 Mar 2003	199	378.5	11.7	742.5	132.2

(more than 50% of the rainfall period is missing) are excluded from the analysis. This procedure resulted in a list of 28 rainfall periods for the study record. Table 1 presents the main characteristics of the rainfall periods.

3.2. Radar Ground Clutter and Beam Blockage Procedures

[11] Two major difficulties of radar rainfall estimation in mountainous regions are signal contamination by ground clutter and radar beam blockage. In Israel the problematic regions are the mountain ridge east of the radar (Samaria and Judean Mountains) that is heavily contaminated by ground clutter, and the Jordan Rift valley east of these mountains that is blocked. Additional ground clutter areas surround the radar at a distance of 20–25 km. It should be noted that the radar is not a Doppler system and therefore no clutter filtering is applied within the radar system.

[12] The approach taken here to overcome the above disturbances is to use radar data from variable elevation angles such that the beam centre lays at least a whole beam width plus 500 m above the ground, and has a negligible beam occultation. The computation of the minimal appropriate radar elevation angle utilizes the 3 arc sec (about 90 m) digital elevation model (DEM) of the U.S. National Oceanic and Atmospheric Administration and it assumes standard propagation conditions. The actual elevation angle used in the analysis is the one that is equal (or closest from above) to the computed one. The results of the described procedure were compared with results obtained using radar data only from the first elevation. The results are described in section 4.4, which shows that it is worthwhile to apply the DEM-based procedure presented in this section.

3.3. Radar Rainfall Estimation Methods: Adjustment Techniques

[13] Radar rainfall estimation methods examined in this study are based on a single power law transformation as a first step and then on the derivation of the rainfall period's radar-to-gauge ratio to adjust the initial estimate. Z is the radar reflectivity (in mm^6m^{-3}) and R the rainfall intensity (in mm/h). The power law derived using the exponential fit proposed in equations (1) and (3) of the famous paper by *Marshall and Palmer* [1948] is $Z = 296R^{1.47}$. We have used:

$$Z = 316R^{1.5} \tag{1}$$

that has been retrieved using 7 a of measurements in central Europe by *Doelling et al.* [1998]. However, it should be noted that while the exponent parameter in the above relationship has some effect on the results, the multiplicative parameter is compensated by the three adjustment techniques described below.

[14] Prior to any processing, the Mekorot radar reflectivity values were increased by 6 dB to compensate system losses not thoroughly taken into account in the ''traditional'' radar equation. A lower threshold of 16 dBZ (dBZ = 10 * Log_{10} Z) for noise filtering and an upper threshold of 65 dBZ are applied to prevent overestimations caused by wet hail particles in the cloud.

[15] Radar rain intensities are cumulated over each rainfall period to get a first guess of the accumulated rain depth estimations, P_i^* (in mm), at the radar pixel above the gauge itself.

[16] Three methods based on adjustment factor are examined:

[17] 1. In the bulk adjustment method [e.g., *Wilson*, 1970; *Brandes*, 1975; *Caine and Smith*, 1976; *Wilson and Brandes*, 1979; *Krajewski and Smith*, 2002], the adjustment factor is constant over the entire study area. The "overall" adjustment is computed over the whole training data set and is defined as the total precipitation amounts as seen by the radar divided by the total of precipitation amounts measured by the gauges:

$$F = \frac{\sum_{i=1}^{N} P_i^*}{\sum_{i=1}^{N} G_i} \tag{2}$$

where G_i (in mm) is the cumulated rain depth for the ith gauge, and, N is the number of gauges in the training data set. Then the "correction" factor applied to radar estimates is simply $1/F$ over the entire region. A logarithmic transformation is often used to make this numeric scale symmetric and linear. The two other methods explained below are based on locally varied adjustment factor. The radar-to-gauge ratio is analyzed on a logarithmic, decibel scale:

$$F_{db}^i = 10\mathrm{Log}_{10}\left(\frac{P_i^*}{G_i}\right) \tag{3}$$

[18] 2. In the weighted regression (WR) method, for the ith radar-gauge couple, the relationship is between the dependent variable $F_{\mathrm{db}}^{\mathrm{i}}$ and the logarithm of the distance from the radar site in reference to a 60 km distance: $\mathrm{Log}D = \mathrm{Log}_{10}(d/60)$, where d is distance from the radar in km. This independent variable represents the well-known range-dependent error in the radar estimation resulted from the beam broadening and its increasing height with distance. By means of the logarithmic transformation we are seeking for a power law dependency. Using a similar approach based on the first spaceborne radar as a reference (instead of gauges), *Gabella et al.* [2006] found a remarkable apparent decrease of sensitivity with range of the ground-based radar. The formula of the WR adjustment is:

$$10\mathrm{Log}_{10}\left(\frac{P^*}{G}\right) = F_{dB} = a_0 + a_D\mathrm{Log}D \tag{4}$$

Gabella et al. [2001] suggested using weighted regression instead of the ordinary regression to derive radar-to-gauge ratios. The regression residuals are weighed according to the physical quantity of interest, i.e., rainfall amounts, in hydrological applications. There is more than one possibility: the weights can be either the radar-derived precipitation amounts or the amount of rain measured by the gauges. More meaningful results are obtained if the values derived from the sensor that has to be adjusted are used for weighting, since the weights act as "soft" thresholds in the regression; less importance is given to those areas where the sensor is "lacking." This fact has already been observed in similar analyses using weighted multiple regressions [*Gabella et al.*, 2001]. Furthermore, it was shown that the best results are obtained when radar-derived rainfall estimates serve as weights for the analysis. Effective clutter suppression is crucial before this kind of weighting [see, e.g., *Gabella et al.*, 2000, Tables 8a and 8b].

[19] 3. In the weighted multiple regression (WMR) method, the technique grasps the spatial variability of the radar-to-gauge ratio (on a decibel scale) through a weighted multiple regression. This adjustment technique was introduced in the Western Alps [*Gabella et al.*, 2000], where it was based on three explanatory variables and made use of full volume 3-D data. It was successful using both maximum reflectivity echoes along the vertical [e.g., *Gabella*, 2004] and "vertical reflectivity profile extrapolated" radar-derived estimates [*Gabella et al.*, 2005], which is the so-called RAIN product by MeteoSwiss in which the "best" estimate of precipitation at ground level is retrieved through a weighted mean of all the radar observations aloft. The three independent variables used were the logarithm of the distance, Log$D$; the height of the ground, H; the minimum height a meteorological target must reach over the gage to be visible to the radar; *HV*. In the current study a similar approach is applied with a simple modification: we have substituted *HV* with the latitude in degrees with reference to the radar location of 32°N: $L = l - 32$ (l is latitude in decimal degrees). Latitude is expected to be correlated with the height of the zero degree isotherm in the studied region and therefore is considered as a factor affecting the radar-to-gauge ratio. The decreasing height of the isotherm with latitude in the Israeli and other regions of climate transition are shown for example by *Harris et al.* [2000, see, e.g., Figure 3, p. 4140]. Note that the three independent variables are "normalized" using intermediated reference values (namely, the selected reference values are 60 km for distance, 0 km for ground height and 32° for latitude). The main advantage of using latitude, L, instead of *HV* is the smaller degree of multicolinearity, which is the condition where one explanatory variable is closely related to another [e.g., *Mosteller and Tukey*, 1977, pp. 280–287]. For the quality-checked gauges used in the training data set, the square of the correlation coefficient between Log$D$ and *HV* is 0.9! The square of the correlation coefficient between Log$D$ and L is instead 0.43. Much smaller values are between Log$D$ and height of ground, H (0.11) and between L and H (0.01). When the purpose of the analysis is to make inferences about the coefficients, there is strong concern about multicolinearity. However, concern about multicolinearity is less when only the predictions are of interest: this is just the case of the following sections 3.4 and 4.2, which deal with the validation of the adjustment techniques. The formula of the WMR adjustment is:

$$10\mathrm{Log}_{10}\left(\frac{P^*}{G}\right) = F_{dB} = a_0 + a_D\mathrm{Log}D + a_H H + a_L L \tag{5}$$

3.4. Training and Validation Procedures

[20] Eleven 20 × 20 km^2 validation areas were defined for the analysis (Figure 2) representing different climate regimes, terrain complexity and distance from the radar site. Table 2 presents characteristics of the validation areas and the number of rain gauges in each area. The total number of gauges in the validation areas is 125.

[21] Training is done for each rainfall period by computing the radar-to-gauge ratios according to the above meth-

Table 2. Characteristics of Validation Areas

Label	Number of Available Gauges	Mean Distance From the Radar	Mean Height of Gauges	Mean Radar Beam Height	Annual Rain[a]	Climate Regime
V1	15	112 km	128 m	2637 m	688 mm	Mediterranean
V2	9	119 km	148 m	2918 m	546 mm	Mediterranean
V3	18	79 km	120 m	2104 m	579 mm	Mediterranean
V4	18	51 km	42 m	1574 m	595 mm	Mediterranean
V5	17	23 km	49 m	1025 m	586 mm	Mediterranean
V6	12	34 km	663 m	1881 m	549 mm	Mediterranean
V7	12	40 km	71 m	1302 m	453 mm	Mediterranean
V8	9	76 km	−36 m	2244 m	342 mm	dry
V9	7	73 km	288 m	2244 m	227 mm	dry
V10	5	89 km	105 m	2007 m	231 mm	dry
V11	3	115 km	357 m	2772 m	110 mm	dry

[a]Climatological annual rain based on 30-a average.

ods based on data in the training data set, which is constructed from 59 gauges located outside the validation areas (Figure 2). Because of the ratio and logarithmic operations (see equation (3)), only nonzero gauge and radar rain depth data are dealt with. In addition, although ground clutter and beam blockage correction procedures are applied (section 3.2 above) to ensure high-quality data in the training data set [*Steiner et al.*, 1999], gauges located in radar pixels that were cluttered or blocked prior to the procedure application are removed from the training data set. However, gauges with similar problematic characteristics were kept in the validation data set.

[22] Coefficients for the three above adjustment methods obtained from the training data set for each rainfall period are then evaluated for the same period in the eleven independent validation areas. This training-validation scheme represents a situation whereby gauge data are available for the rainfall period at hand (non-real-time application). To quantify the goodness of quantitative precipitation estimation we use the N independent gauges (see column 2 in Table 2) available in each validation area. The comparison between gauge accumulated rain depth, G_i (mm), and the corresponding precipitation amount, P_i (mm), which was derived from radar observation aloft, is based on the following scores: (1) bias,

$$\frac{\sum_{i=1}^{N} P_i}{\sum_{i=1}^{N} G_i}$$

(analyzed on a logarithmic, decibel scale), and (2) fractional standard error (FSE),

$$\frac{\sqrt{\frac{1}{N}\sum_{i=1}^{N}(P_i - G_i)^2}}{\frac{1}{N}\sum_{i=1}^{N} G_i}.$$

[23] To judge the validation results, a reference level of error is computed in the form of gauge-only estimation. For each gauge in the validation areas, the corresponding accumulated depth for the rainfall period is computed by spatial interpolation of gauge data of the independent training data set. Note that these gauges are located outside the validation areas. In this work, two interpolation methods are used. One is the standard Inverse Distance Weight (IDW) with power of two and the second is the universal Kriging technique. If the radar-derived QPE (from echoes aloft) results in better scores than the gauge-derived QPE (from measurements outside the validation area itself), then radar-adjusted echoes (in ungauged areas) are considered useful.

4. Results

4.1. Five-Year Analysis: Training Data Set

[24] The analysis was applied to the twenty eight rainfall periods obtained from the 5-a record. It is not surprising that, in the presence of hills, mountains and shielded regions, radar precipitation estimates derived aloft using a single Z-R relationship (independently also of the height of Z) result in underestimation. Radar underestimation is the effect of a decreasing vertical profile of reflectivity with height, combined with beam shielding and/or occultation by relief.

[25] As already stated, the so-called bulk adjustment is the simplest remedy that can be used to compensate for the bias. It consists in multiplying radar precipitation estimates by the ratio between the gauges and radar total (overall total, in time and space). If we include the 28 rainfall periods the overall bias is computed to be −2.1 dB. It means that, on average, radar-derived amounts should be multiplied by 1.62 to correct bias relative to gauges. This value is probably the effect of relief, obstacles and shielding. Consider that in a complex orographic region such as the Western Alps, despite the use maximum reflectivity echoes, *Gabella and Notarpietro* [2004] found an overall bias of −4 dB.

[26] Using the same sets of 28 rainfall periods and radar-gauge couples, the two WR-derived coefficients resulted to be (average ± standard deviation):

$$F_{dB} = -(1.5 \pm 1.7) - (6.2 \pm 1.9) \cdot \mathrm{Log}D \qquad (6)$$

[27] If the variability of the radar-to-gauge ratio, F_{dB}, explained by the independent variable, Log$D$, were small, the bulk adjustment technique would be equivalent to the WR adjustment. This is not the case: hence we expect this

Table 3. Weighted Fractional Standard Error for the 28 Rainfall Periods[a]

	Radar-Derived Rainfall Amounts			Gauge-Derived Rainfall Amounts	
	Bulk Adjustment	WR Adjustment	WMR Adjustment	Kriging	IDW
V1[b]	0.78[c]	0.72[c]	0.72[c]	1.14	**0.24**
V2[b]	0.69[c]	0.62[c]	0.61[c]	1.13	**0.21**
V3	0.36	0.34	0.34	1.01	**0.16**
V4	0.93[d]	0.45	0.41	1.13	**0.21**
V5	1.80[c]	0.32[d]	0.32	1.11	**0.25**
V6	0.80	0.51	0.49	0.90[d]	**0.30**
V7	0.80[d]	0.22[d]	**0.19**	0.93[d]	0.30
V8	0.47	**0.42**	0.47	1.05	0.60[d]
V9	0.38	0.33	**0.30**	0.82	0.50[d]
V10	0.29	0.37	**0.21**	1.09	0.34
V11[b]	0.47	0.56	**0.46**	0.95	4.42[c]

[a]Boldface indicates lowest FSE value.
[b]Range is larger than 100 km.
[c]Bias is not within ±3 dB.
[d]Bias is not within ±1.2 dB.

simple, isotropic, range adjustment to perform better than a constant factor for the whole surveillance area. It is significant that the coefficient a_D which relates F_{dB} to Log$D$, is negative for all the 28 rainfall periods. This confirms previous results obtained using the TRMM spaceborne radar as a reference instead of gauges (M. Gabella et al., Combining multisource non-conventional observations of the precipitation field in the southeastern Mediterranean area, submitted to *Atmospheric Research*, 2006): the Shacham radar underestimates rainfall amounts at longer distances. Note that similar results have been previously obtained also in Cyprus [*Gabella et al.*, 2006].

[28] For the same data sets, the four WMR-derived regression coefficients resulted to be (average ± standard deviation):

$$F_{dB} = -(1.0 \pm 1.8) - (5.3 \pm 2.0) \cdot \mathrm{Log}D - (2.0 \pm 2.5) \cdot H - (0.4 \pm 1.4) \cdot L \quad (7)$$

[29] Thanks to the WMR, radar-derived rainfall amounts are not equally amplified over the whole region; instead, each radar pixel receives a correction factor that is a function of the distance from the radar, of the altitude and latitude. Note also, that while the WR adjustment is isotropic with respect to the radar site, the WMR adjustment is not.

[30] As expected, the coefficient a_D is negative. This confirms previous results obtained on both sides of the Western Alps [*Gabella*, 2004; *Gabella et al.*, 2005] and in Nordic countries [*Michelson and Koistinen*, 2000].

[31] The values of the coefficients are somewhat artificial, since they depend on the units that are used in the regression and on the reference system (difference in heights are in km with respect to mean sea level; differences in latitude are angular values in degrees with respect to the 32° parallel; the ratio in distances, before the logarithmic transformation, is with respect to an intermediate value of 60 km). Further-

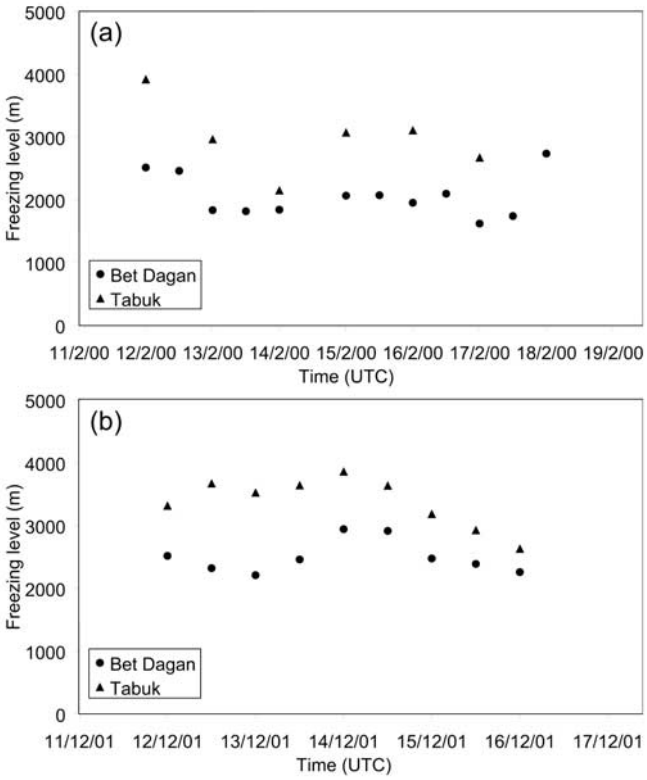

Figure 3. Freezing level computed from sounding data for the Bet Dagan station in Israel (coordinates: 34.81°E/32.00°N) and the Tabuk station in Saudi Arabia (coordinates: 36.60°E/28.28°N), for two rainfall periods: (a) 12–17 February 2000 and (b) 12–15 December 2001.

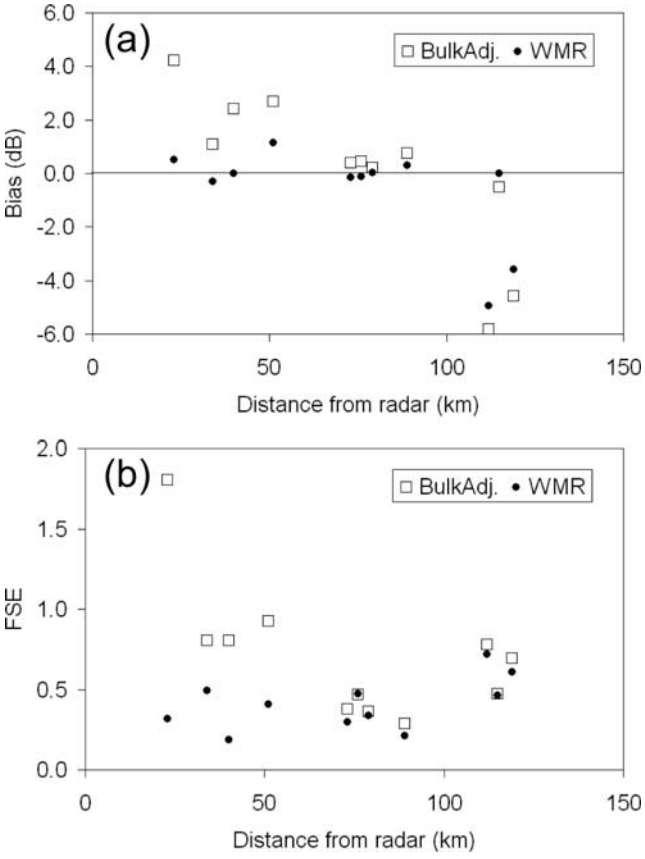

Figure 4. Errors (weighted averages) in terms of (a) bias and (b) FSE of radar estimates as a function of distance from the radar for the bulk adjustment and WMR methods.

more, the regression coefficients should be applied only within the range they were determined (e.g., distances between 9 and 148 km, the nearest and farthest gauges available in the regression, latitude between 30.77° and 33.77°, altitudes between 390 m below sea level and 960 m above). Hence the value of the offset, a_0, represents the value of F_{dB} at 60 km from the radar and on a hypothetic site where the altitude is 0 m and the latitude 32°. We avoid making further inferences about the coefficients because of multicolinearity, especially between Log$D$ and L (see section 3.3 for more details).

4.2. Five-Year Analysis: Validation Using Independent Data Sets

[32] Gauges within the eleven validation areas were not included in the training procedure so that their data can be used to independently validate the rainfall estimates. The scores defined at the end of section 3.4 (bias and, most of all, FSE) are used to assess the performances of the gauge-adjusted radar rainfall estimates in independent areas (Table 3). The presented scores are the weighted averages of the 28 individual scores for each rainfall period with the average rain depth (i.e., column 5 in Table 1) as weights. These scores, which characterize radar-derived estimates, are compared with a "reference level of error." This reference consists of spatial interpolation of gauge data in the training data set. The Inverse Distance Weight (IDW) and the Kriging methods are used for the interpolation.

[33] For the sake of conciseness, we show in Table 3 only the weighted average of FSE and not also the bias, which is much less variable. Because of the adjustment, in fact, the bias is in most of the cases close to the ideal value of 0 dB. There are some exceptions: if the bias is not within ±1.2 dB, the corresponding FSE value is tagged with footnote d. In some desperate cases, which are flagged with footnote c, the bias is not within ±3 dB (a factor of 2) even after the adjustment based on the training data set.

[34] For all the Mediterranean validation areas the WR and WMR adjustments performing better than the bulk adjustment. Gauge interpolation provides better estimates in these areas, except for V7 (the most southern one). For the five validation areas that are less than 100 km distance from the radar (V3–V7), the FSE of the WMR method is within a reasonable range of 20–50% with biases from −0.3 to 1.1 dB (−7 to +30%).

[35] For the two distant Mediterranean validation areas V1 and V2 a significant underestimation of the radar-based rainfall methods is presented and the errors in terms of FSE are relatively large. Most probably the cause of the radar underestimation in these areas is the great distance from the radar system (more than 100 km) that causes an overshoot of radar beam above precipitation in these areas (on average radar beam is more than 2.6 km above sea level, Table 2).

[36] For all four dry climate validation areas (V8–V11), gauge-adjusted radar-derived estimates are considerably better than gauge interpolation. The WR and WMR adjustment are again better than a simple bulk adjustment. The bias of the WMR method ranges from −0.1 to 0.3 dB (−3 to +8%). Not surprisingly, gauge interpolation methods in these areas resulted in poor estimation of rainfall because of the insufficient density of rain gauge network (many of the gauges in the training data set are, in fact, relatively close to the Mediterranean validation areas while only few are near the dry areas), while the radar-based methods provided still reasonable results.

[37] It is interesting to note that the radar estimates for validation area V11 at 115 km mean distance from the radar and mean beam altitude of almost 2.8 km above sea level do not present the severe underestimates shown in the distant Mediterranean areas V1 and V2. We assume that the difference between the two regions is in the freezing level height, which generally increases from north to south. This gradient is demonstrated in Figure 3 for two of the analyzed rainfall periods (12–17 February 2000 and 12–15 December 2001) by plotting the freezing level computed from sounding data for the Bet Dagan station in Israel (coordinates: 34.81°E/32.00°N, 8 km west to radar location, see Figure 2) and the Tabuk station in Saudi Arabia (coordinates: 36.60°E/28.28°N). Climatological evidence of the remarkable north-to-south freezing level increase at latitudes close to Shacham radar surveillance area (∼31–33°N) during winter months is shown for example by *Harris et al.* [2000, see, e.g., Figure 10, p. 4146].

[38] From a subjective evaluation based on Table 3 we conclude that the scores of the WMR seem to be slightly better than the scores of the WR, especially for what concerns FSE in the dry validation areas V10 and V11 and the bias in the Mediterranean areas V5 and V7.

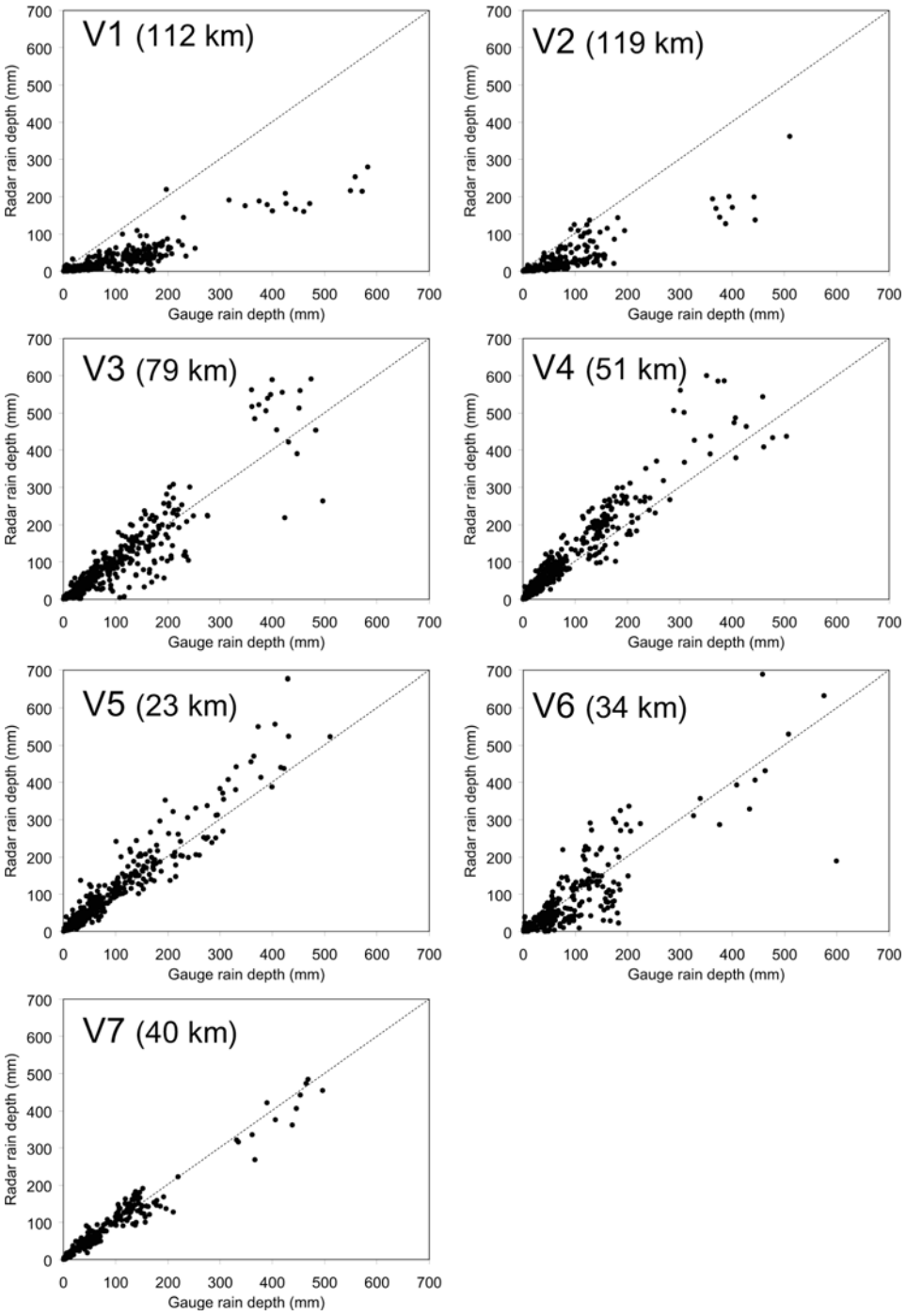

Figure 5. Fit between accumulated rain depth over rainfall periods derived from gauge and from radar for the seven Mediterranean validation areas V1–V7. Mean distance from radar is indicated in parentheses.

[39] Comparison of the bulk adjustment and the WMR radar estimation methods in terms of range-dependent errors is presented in Figure 4. Figure 4 presents the FSE and bias scores (weighted averages for the individual rainfall periods) as a function of distance from radar for the WMR adjustment and the bulk adjustment. As can be seen, the WMR method almost completely removes this source of error in the radar estimates within the 100 km range.

[40] The fit between point measurements and the WMR-adjusted radar-derived estimates is represented in Figures 5 and 6 in the form of scatterplots (rain depth for the individual rainfall periods). Figure 5 shows the fit for the seven Mediterranean validation areas, and it can be seen that systematic underestimation occurs for the long-range validation areas V1 and V2 in the north (as mentioned above). Figure 6 refers to the dry validation areas. Note the differences in the maximum values in the x and y axes: in V8 in

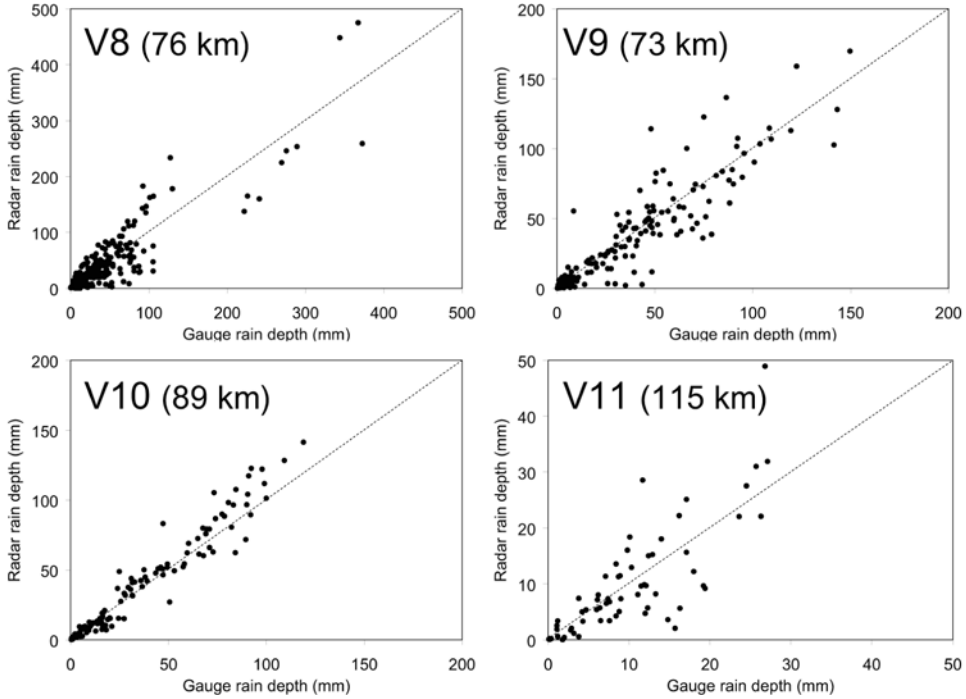

Figure 6. Fit between accumulated rain depth over rainfall periods derived from gauge and from radar for the four dry climate validation areas (V8–V11). Mean distance from radar is indicated in parentheses.

the north (close to Jordan and Syria) almost 400 mm were measured in three cases, all related to the same rainfall period. For the two drier areas V10 and V9 "large values" are between 100 and 150 mm, while for the arid area V11 it is between 20 and 30 mm. These significant differences in the largest accumulated rain depth values are also reflected in the climatological annual rainfall of the validation areas (see Table 2 and Figure 2a).

[41] Adding up, in 9 areas (latitude between 30.5°N and 33°N) out of 11, radar-derived WMR-adjusted amounts

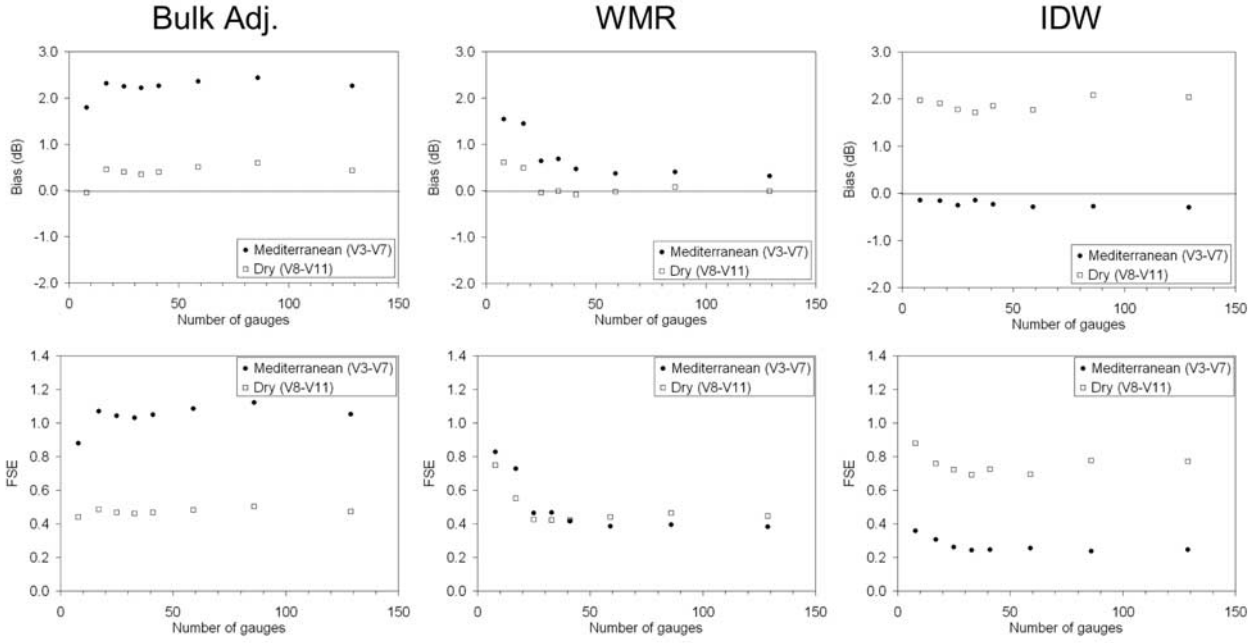

Figure 7. Effect of number of gauges in the training data set on bias and FSE for the two groups of climate regimes (Mediterranean and dry) and for the two radar estimate methods (bulk adjustment and WMR).

Table 4. Weighted FSE for Validation Areas Using Data From the Lowest Radar Elevation Angle

	Bulk Adjustment	WMR Adjustment
V1[a]	0.78[b]	0.68[b]
V2[a]	0.70[b]	0.60[c]
V3	0.45	0.47
V4	0.65	0.52
V5	2.49[b]	0.57
V6	2.39[c]	1.16
V7	0.54[c]	0.31
V8	0.60[b]	0.61[b]
V9	0.67[c]	0.40
V10	0.27	0.43
V11[a]	0.48	0.72

[a]Range is larger than 100 km.
[b]Bias is not within ±3 dB.
[c]Bias is not within ±1.2 dB.

provided good estimates. In 5 of them, the WMR amounts were the best estimates. WMR-adjusted radar estimates were the best in three dry validation areas (V9–V11), despite the relatively large distance (average distances are 76, 89 and 115 km). Gauge interpolation provided better estimates for 6 out of the 7 Mediterranean validation areas.

[42] In general, a good fit is achieved between the gauge and radar rain depth for 28 relevant rainfall periods in the 5 a of data. We conclude that the radar system can be used for quantitative precipitation estimation, at least in the entire western and northeastern parts of Israel in regions that are less than 100 km distance of the radar.

4.3. Sensitivity Analysis: Number of Gauges in the Training Data Set

[43] The above results were obtained using a set of 59 rain gauges in the training data set. The total number of gauges available (outside of the validation areas) is 129. Here, we examine the effect of gauge density in the training data set on error in validation areas. The validation areas were grouped into two categories, depending on their climate regime (Mediterranean or dry, see last column of Table 2). The two areas with significant underestimations (V1 and V2) were removed from this analysis. Figure 7 presents the effect of number of gauges between 8 and 129 on bias and FSE for the two groups. These results indicate that applying the WMR method, 40 gauges (average density of one gauge per 587 km^2) are more or less sufficient to achieve a stable error. Fewer gauges resulted in an increase of errors with overestimations of the radar rainfall estimates. Low sensitivity to gauge number is evident for the bulk adjustment method. Rainfall estimates based on gauge interpolation may also be sensitive to the number of gauges. As shown in Figure 7, also for the IDW method from 40 gauges and up the error is the practically same. It should be emphasized that the levels of errors presented in Figure 7 are the weighted averaged FSE and bias scores. The same analysis conducted for individual rainfall periods resulted in higher sensitivity to gauge number (not shown).

4.4. Sensitivity Analysis: Using a Fixed Lowest Elevation

[44] Additional sensitivity analysis was conducted to examine the advantage of the radar ground clutter and beam blockage procedures described in section 3.2. What happens if instead of using the first clutter-free and/or nonshielded elevation we use a fixed one? Results with the lowest elevation at $\sim 0.8^\circ$ clearly show that the two closest validation areas (V5 and V6) are so affected by ground clutter that it causes a severe bias and FSE. To avoid this, bias and FSE were subsequently computed for a subgroup of gauges located in high-quality radar pixels. Table 4 presents weighted FSE values for these gauges. The comparison with Table 3 reveals that it is worthwhile to apply the GIS-based procedure described in section 3.2, which simply requires a DEM of the region and is based on the assumption of standard atmospheric refractivity and geometric optics. The GIS-based procedure that selects the "first-usable" lowest elevation is better than a fixed lowest elevation even when only high-quality pixels are considered.

5. Summary and Conclusions

[45] The use of radar for quantitative precipitation estimation in Israel was analyzed in this study. The area is characterized by different climate regimes (Mediterranean to dry) and topographic conditions. The analysis optimized radar-derived accumulated rain depth values during rainfall periods (i.e., successive rainy days) with three gauge adjustment methods: a one-coefficient bulk adjustment, a two-coefficient weighted regression (WR), and a four-coefficient weighted multiple regression (WMR). The first removed the mean bias from the radar estimates while the two others were based on a local correction. The WR method considers the single factor of distance from radar and the WMR method considers three factors: distance from radar, elevation and latitude. A training set of 59 independent, quality-checked gauges was used for each rainfall period and independent sets containing 125 gauges spread over 11 validation areas were used for the evaluation.

[46] Comparison of the radar-based gauge adjustment methods revealed that WR and WMR always perform better than the bulk adjustment with a slight better performance of the latter. In distances of up to 100 km from the radar, the "error" in WMR-adjusted estimates shows weighted FSE values between 0.21 and 0.49 (while the bias is within 30%). In northern areas with distance more than 100 km from the radar, a considerable underestimation is detected and the error is much larger. On the other hand, for a far southern area, radar rainfall estimates are still "good" (FSE < 0.49), which is presumably related to higher freezing levels in the south compared to northern Israel. It is shown that the above-mentioned levels of error could be achieved with a training data set of 40 gauges or more.

[47] Moreover, in this study we assessed the errors in radar rainfall estimates by comparing it to a reference level of error. This was the error obtained on the basis of gauge-only data. Rainfall estimation for the gauge points within the validation areas were derived applying spatial interpolation (IDW and Kriging) of gauge data in the training data set. Note that these gauges are outside the validation areas. In this approach, radar-based rainfall estimates provide useful information if it reduces the level of errors in

gauge-only estimates. In all dry validation areas and in the most southern Mediterranean area, radar-based estimates were remarkably better than gauge-only estimates. However, for six Mediterranean validation areas, the radar estimates are inferior relative to the gauge interpolation estimates.

[48] We conclude that the radar-based WR and WMR adjustment methods provide good quantitative accumulated rain depth estimation in ungauged areas up to 100 km north and about 120 km south of the radar system. Areas east and southeast of the radar (e.g., the Dead Sea region) were not examined because of insufficient gauge data. It should be emphasized that the validation areas were located throughout the radar coverage area in which gauge data were available for comparison, including ''problematic'' areas prone to ground clutter and beam blockage errors. The procedure developed here to overcome these errors makes use of radar data from optimal elevation angles that are varied in space. This is a similar approach to the hybrid scan method applied by the U.S. national weather service [*Fulton et al.*, 1998] for the NEXRAD radar network system. Because of the relatively large coverage radar area examined and the large number of rainfall periods we believe the methodology presented here can be used operationally. It should be clear; however, that this methodology is currently based on daily gauge data that are provided after the storm and therefore it is not a real-time estimation method but allows after-case analysis.

[49] In addition, attention should be paid to the different meaning of point and areal rainfall amounts. In the present study, comparisons are conducted between point gauge data and radar rainfall in pixels above these points. For such comparisons, differences in rainfall attributed to the differences in domain size (30 m^3 versus 2–6 km^3) are incorrectly interpreted as radar estimation errors. When areal rainfall is of interest, e.g., for hydrological applications, representative ground truth data are not available because of the typically low gauge density. Therefore the assessment of the errors in radar-based QPE is difficult. Moreover, it is possible that errors in the gauge-based areal rainfall estimates are even larger than radar-based gauge-adjusted estimates. An indication for that can be seen in the comparisons between gauge interpolation and radar estimates shown in this study. The estimation of areal rainfall is, however, not the scope of this paper and requires further investigation.

[50] **Acknowledgments.** Radar data were provided by E.M.S Mekorot, and gauge data were provided by the Israel Meteorological Service. Partial funds for the research project were provided by the Israel Science Foundation (grant 880/04), the Israel Ministry of Science and Technology and the Israel National Water Commissioner. Special thanks are due to Urs Germann and Jürg Joss for helpful suggestions and stimulating discussions. One author (M.G.) has visited the Hebrew University in October 2006 thanks to the Vigevani Prize for Academic Exchange. The authors would like to thank the three anonymous reviewers for their valuable and stimulating comments and Simon Berkovich for his help in manuscript editing.

References

Ahrens, C. D. (2003), *Meteorology Today: An Introduction to Weather, Climate, and the Environment*, 7th ed., Brooks/Cole-Thomson Learning, Pacific Grove, Calif.

Brandes, E. A. (1975), Optimizing rainfall estimates with the aid of radar, *J. Appl. Meteorol.*, *14*, 1339–1345.

Caine, D. E., and P. L. Smith (1976), Operational adjustment of radar estimated rainfall with rain gauge data: A statistical evaluation, in *Preprints of the 17th Conference on Radar Meteorology*, pp. 533–538, Am. Meteorol. Soc., Seattle, Wash.

Collier, C. G. (1986), Accuracy of rainfall estimates by radar, part I: Calibration by telemetering rain gauges, *J. Hydrol.*, *83*, 207–223.

Collier, C. G., P. Larke, and B. May (1983), A weather radar correction procedure for real-time estimation of surface rainfall, *Q. J. R. Meteorol. Soc.*, *109*, 589–608.

Doelling, I. G., J. Joss, and J. Riedl (1998), Systematic variations of Z-R relationships from drop size distributions measured in Northern Germany during seven years, *Atmos. Res.*, *48*, 635–649.

Fulton, R. A., J. P. Breidenbach, D. J. Seo, and D. A. Miller (1998), The WSR-88D rainfall algorithm, *Weather Forecasting*, *13*, 377–395.

Gabella, M. (2004), Improving operational measurement of precipitation using radar in mountainous terrain–Part II: Verification and applications, *IEEE Geosci. Remote Sens. Lett.*, *1*, 84–89.

Gabella, M., and R. Notarpietro (2004), Improving operational measurement of precipitation using radar in mountainous terrain–Part I: Methods, *IEEE Geosci. Remote Sens. Lett.*, *1*, 78–83.

Gabella, M., J. Joss, and G. Perona (2000), Optimizing quantitative precipitation estimates using a non-coherent and a coherent radar operating on the same area, *J. Geophys. Res.*, *105*, 2237–2245.

Gabella, M., J. Joss, G. Perona, and G. Galli (2001), Accuracy of rainfall estimates by two radars in the same Alpine environment using gauge adjustment, *J. Geophys. Res.*, *106*, 5139–5150.

Gabella, M., M. Bolliger, U. Germann, and G. Perona (2005), Large sample evaluation of cumulative rainfall amounts in the Alps using a network of three radars, *Atmos. Res.*, *77*, 256–268.

Gabella, M., J. Joss, S. Michaelides, and G. Perona (2006), Range adjustment for ground-based radar, derived with the space borne TRMM Precipitation Radar, *IEEE Trans. Geosci. Remote Sens.*, *44*, 126–133.

Germann, U., and J. Joss (2004), Operational measurement of precipitation in mountainous terrain, (Chapter 2) in *Weather Radar: Principles and Advanced Applications*, edited by P. Meischner, *Phys. Earth Space Environ.*, vol. 17, ch. 2, pp. 52–77, Springer, New York.

Goldreich, Y. (2003), *The Climate of Israel, Observations, Research and Applications*, 298 pp., Springer, New York.

Goodrich, D. C., J. M. Faures, D. A. Woolhiser, L. J. Lane, and S. Sorooshian (1995), Measurement and analysis of small-scale convective storm rainfall variability, *J. Hydrol.*, *173*(1–4), 283–308.

Harris, G. N., Jr., K. P. Bowman, and D. Shin (2000), Comparison of freezing-level altitudes from the NCEP reanalysis with TRMM Precipitation radar brightband data, *J. Clim.*, *13*(23), 4137–4148.

Joss, J., and A. Waldvogel (1990), Precipitation measurements and hydrology, A review, in *Radar Meteorology*, edited by D. Atlas, pp. 577–606, Am. Meteorol. Soc., Boston, Mass.

Kahana, R., B. Ziv, Y. Enzel, and U. Dayan (2002), Synoptic climatology of major floods in the Negev Desert, Israel, *Int. J. Climatol.*, *22*, 867–882.

Kitchen, M., and R. M. Blackall (1992), Representativeness errors in comparisons between radar and gauge measurements of rainfall, *J. Hydrol.*, *134*, 13–33.

Koistinen, J., and T. Puhakka (1981), An improved spatial gauge-radar adjustment technique, in *Preprints of the 20th Conference on Radar Meteorology*, pp. 179–186, Am. Meteorol. Soc., Boston, Mass.

Krajewski, W. F., and J. A. Smith (2002), Radar hydrology: Rainfall estimation, *Adv. Water Resour.*, *25*, 1387–1394.

Krajewski, W. F., G. J. Ciach, and E. Habib (2003), An analysis of small-scale rainfall variability in different climatological regimes, *Hydrol. Sci. J.*, *48*(2), 151–162.

Marshall, J. S., and W. M. Palmer (1948), The distribution of raindrops with size, *J. Meteorol.*, *5*, 165–166.

Michaud, J. D., and S. Sorooshian (1994), Effect of rainfall-sampling errors on simulations of desert flash floods, *Water Resour. Res.*, *30*(10), 2765–2775.

Michelson, D., and J. Koistinen (2000), Gauge-radar network adjustment for the Baltic Sea experiment, *Phys. Chem. Earth, Part B*, *25*, 915–920.

Morin, E., R. A. Maddox, D. C. Goodrich, and S. Sorooshian (2005), Radar Z-R relationship for summer monsoon storms in Arizona, *Weather Forecasting*, *20*(4), 672–679.

Mosteller, F., and J. Tukey (1977), *Data Analysis and Regression*, Addison Wesley, Boston, Mass.

Seo, D. J., J. P. Breidenbach, R. Fulton, D. Miller, and T. O'Banon (2000), Real time adjustment of range dependent biases in WSR-88D rainfall estimates due to non-uniform vertical profile of refractivity, *J. Hydrometeorol.*, *1*, 222–224.

Smith, J. A., and W. F. Krajewsky (1991), Estimation of the mean field bias of radar rainfall estimates, *J. Appl. Meteorol.*, *30*, 397–412.

Steiner, M., J. A. Smith, S. J. Burges, C. V. Alonso, and R. W. Darden (1999), Effect of bias adjustment and rain gauge data quality control on radar rainfall estimation, *Water Resour. Res.*, *35*, 2487–2503.

Wilson, J. W. (1970), Integration of radar and gauge data for improved rainfall measurements, *J. Appl. Meteorol.*, *9*, 489–497.

Wilson, J. W., and E. A. Brandes (1979), Radar measurement of rainfall–A summary, *Bull. Am. Meteorol. Soc.*, *60*, 1048–1058.

M. Gabella, Dipartimento di Elettronica, Politecnico di Torino, I-10129 Turin, Italy.

E. Morin, Department of Geography, Hebrew University of Jerusalem, Jerusalem 91905, Israel. (msmorin@mscc.huji.ac.il)